ELSEVIER

Journal of Chromatography A, 855 (1999) 291–303

JOURNAL OF CHROMATOGRAPHY A

www.elsevier.com/locate/chroma

Understanding of peak deterioration in hyphenated speciation systems due to gas–liquid separation in the hydride generation interface

Johannes T. van Elteren[a,*], Zdenka Šlejkovec[a,b]

[a]*Department of Radiochemistry, Interfaculty Reactor Institute, Delft University of Technology, Mekelweg 15, 2629 JB Delft, The Netherlands*

[b]*Department of Environmental Sciences, Jožef Stefan Institute, Jamova 39, 1111 Ljubljana, Slovenia*

Received 30 March 1999; received in revised form 31 May 1999; accepted 1 June 1999

Abstract

In hyphenated speciation systems with a hydride generation interface one of the processes influencing peak deterioration is gas–liquid separation. A mathematical model was developed to calculate attenuation, signal tailing and resolution loss of HPLC peaks due to gas–liquid separation. It was shown experimentally — using an HPLC–hydride generation–atomic fluorescence spectrometry system for arsenic speciation — that the mathematical model predicts peak deterioration well. This allowed us to study the parameters influencing the deterioration, viz. gas–liquid separation parameters (gas–liquid separator head space volume and purge gas volume flow-rate) and HPLC peak parameters [width (ratio) and resolution] theoretically, simulating HPLC peaks with gaussian functions.

Keywords: Speciation; Hydride generation; Mathematical models; Gas–liquid separation interface; Arsenic; Metals

1. Introduction

In the last decade considerable progress has been made in elemental speciation research, mainly due to the development of hyphenated systems [1]. Such systems consist of a chromatographic device, gas (GC) or liquid (LC) chromatograph, interfaced with an element-specific detector. As a result of the availability of increasingly sensitive detection methods, especially inductively coupled plasma mass spectrometry (ICP-MS [2]), low-level speciation in environmental, biological and medical applications has become more or less routine using LC-based hyphenated systems [3,4]. However, since ICP-MS equipment is not everywhere directly available for such applications, many researchers have sought intermediate solutions. One of the most favourable solutions is the use of a chemical interface, between a high-performance liquid chromatography (HPLC) system and a quartz furnace atomic absorption spectrometry (QFAAS) system or an atomic fluorescence spectrometry (AFS) system, for volatilisation of the element under study [5]. To this end mostly an on-line hydride generation (HG) unit is used which allows reduction of (certain) compounds of As, Sb, Se, etc. to their corresponding hydrides by sodium

*Corresponding author. Tel.: +31-15-278-6770: fax: +31-15-278-3906.

E-mail address: elteren@iri.tudelft.nl (J.T. van Elteren)

0021-9673/99/$ – see front matter
PII: S0021-9673(99)00691-3

borohydride ($NaBH_4$) under acidic conditions [6]. Compounds not susceptible to hydride generation have to be on-line mineralised in a microwave (MW) or ultraviolet (UV) decomposition unit before their reduction with $NaBH_4$. In a gas–liquid separator (GLS) the volatilised compounds are separated from the reaction mixture prior to measurement.

However, on-line sample processing for decomposition and hydride generation may introduce significant peak deterioration. When comparing the resolution characteristics of HPLC–ICP-MS [7,8] with systems such as HPLC–MW-HG–QFAAS [9,10] or HPLC–UV-HG–AFS [11,12] for As speciation, it is noticeable that ICP-MS chromatograms have ''sharper'' peaks. The obvious reason for peak deterioration is dispersion in the decomposition and hydride generation interfaces. By segmenting the reacting sample flow in the decomposition coil with gas bubbles, it has been demonstrated that dispersion can be reduced to a great extent [13]. However, serious dispersion is envisaged since the residence time of hydrides in the head space of the gas–liquid separator — depending on the headspace volume and the gas flow-rates (hydrogen evolved from decomposition of $NaBH_4$ and additional purge gas) — is substantial in almost all applications. Furthermore, the quality of HPLC peaks [width (ratio) and resolution] determine the magnitude of the dispersion.

A better understanding of the parameters influencing peak deterioration due to gas–liquid separation is important for improving the resolution characteristics. Johansson et al. [14] reported a deconvolution method for GC–AAS peaks to improve the accuracy in the quantitation of peaks. In this work an earlier formulated mathematical model for flow injection–HG–AFS [15] was adapted to predict the influence of the gas–liquid separator, i.e. purge gas flow-rate and GLS head space volume, on HPLC peaks. Gaussian functions with varying width (ratio) and resolution were applied to simulate peaks from the HPLC column. Verification of the mathematical model was by separation of a mixture of arsenic compounds in an HPLC–HG–AFS system and comparison of the GLS output peaks generated experimentally and theoretically.

1.1. Formulation of mathematical model

In Fig. 1 an outline of the hyphenated HPLC–HG–AFS speciation system is given (see experimental section for technical details). An analyte species i with concentration c_i (in mol l^{-1}) is injected via a sample loop with volume V_L (in l). Analyte species i passes over the HPLC column with a mass flow-rate $f_{HPLC,i}(t)$ (in mol s^{-1}) and undergoes hydride formation with $NaBH_4$ in the presence of HCl. Assuming a reduction efficiency E_i (between 0 and 1) for analyte species i and negligible signal delay and signal dispersion in the signal transfer from HPLC to GLS, the hydride concentration $c_{GLS,i,in}(t)$ of analyte species i in the gas phase entering the GLS (in mol l^{-1}) can be written as

$$c_{GLS,i,in}(t) = \frac{f_{HPLC,i}(t) \cdot E_i}{F_H} \quad (1)$$

where the hydrogen volume flow-rate F_H (in l s^{-1}) is

$$F_H = 22.4 \cdot 4 \cdot c_{BH} \cdot F_{BH} \quad (2)$$

with c_{BH} the concentration of $NaBH_4$ (in mol l^{-1}) and F_{BH} the volume flow-rate of $NaBH_4$ (in l s^{-1}). When more analyte species i (i between 1 and m) are involved, Eq. (1) may be rewritten as

$$c_{GLS,in}(t) = \sum_{i=1}^{m} c_{GLS,i,in}(t) = \frac{\sum_{i=1}^{m} (f_{HPLC,i}(t) \cdot E_i)}{F_H} \quad (3)$$

with $c_{GLS,in}(t)$ as the overall hydride concentration in the gas phase entering the GLS (in mol l^{-1}).

The hydrides formed from the various analyte species i are separated from the reaction mixture in a GLS, and H_2 and Ar sweep the hydrides from the GLS to the AFS detector via a dryer. The overall hydride concentration $c_{GLS,in}(t)$ undergoes dispersion in the GLS which can be calculated numerically assuming the input signal to be subdivided into blocks yielding a histogram (see Fig. 2, large graph). Each block n_j ($j = 1, 2, \ldots$) with width Δt (in s) can be treated individually as illustrated for block n_7 (see Fig. 2, insert).

In analogy with a model formulated earlier [15] the maximum GLS output of a block n_j, reached at $t = n_j\ \Delta t$, is

$$c_{GLS,out,max}(t = n_j\ \Delta t) = c_{GLS,in}(t = n_j\ \Delta t) \cdot \frac{F_H}{F_H + F_A} \cdot \left(1 - \exp - \frac{F_A + F_H}{V_G} \Delta t\right) \quad (4)$$

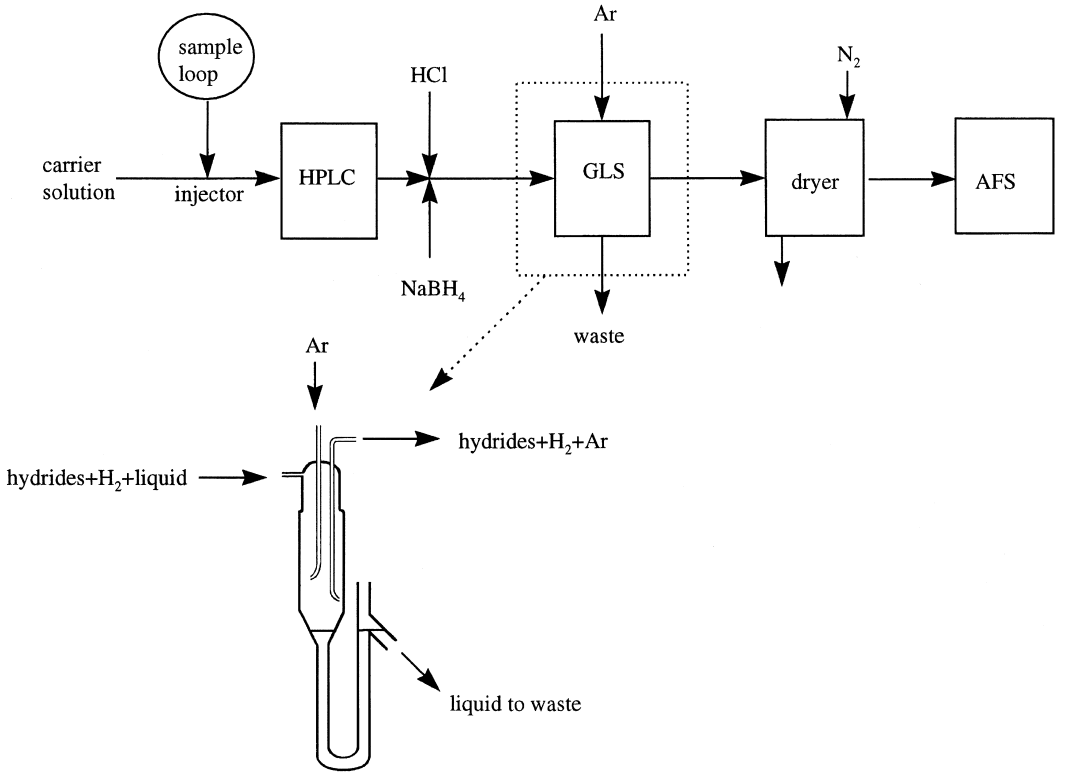

Fig. 1. Schematic diagram of HPLC–HG–AFS system with details of the GLS.

with F_A as the volume flow-rate of argon purge gas (in l s^{-1}) and V_G as the head space volume of the GLS (in l).

The GLS output of block n_j at time $t = n_p\ \Delta t$ with $p=j,\ j+1, \ldots$ can be written as

$$c_{\mathrm{GLS,out},n_j}(t = n_p\ \Delta t) = c_{\mathrm{GLS,out,max}}(t = n_j\ \Delta t) \cdot \exp - \frac{(F_H + F_A) \cdot (p - j)\ \Delta t}{V_G} \quad (5)$$

The general GLS output of histogram $\Sigma_{j=1}^{p}\ n_j$ at time $t = n_p\ \Delta t$ with $p=j,\ j+1, \ldots$ can be obtained by summing all blocks n_j with j from 1 to p giving

$$c_{\mathrm{GLS,out},\sum_{j=1}^{p} n_j}(t = n_p\ \Delta t) = \sum_{j=1}^{p} \left[c_{\mathrm{GLS,out,max}}(t = n_j\ \Delta t) \cdot \exp - \frac{(F_H + F_A) \cdot (p - j)\ \Delta t}{V_G} \right] \quad (6)$$

1.2. Simulation of gaussian type HPLC signals

Ideally, analyte species i separated on an HPLC column have a gaussian type mass flow-rate $f_{\mathrm{HPLC},i}(t)$ of the following type:

$$f_{\mathrm{HPLC},i}(t) = \frac{2\sqrt{2} \cdot V_L \cdot c_i}{w_i \cdot \sqrt{\pi}} \cdot \exp - \frac{8 \cdot (t - t_{R,i})^2}{w_i^2} \quad (7)$$

where $f_{\mathrm{HPLC},i}(t)$ is mass flow-rate of analyte species i in HPLC effluent (in mol s^{-1}), $V_L \cdot c_i$ is total amount of analyte species i injected (in mol), $t_{R,i}$ is retention time of analyte species i (in s) and w_i is width of HPLC peak of analyte species i at 13.5% of peak height (in s).

If we assume that the signal transfer from HPLC to GLS takes place with negligible delay and dispersion (due to minimal tubing diameter), Fig. 3 illustrates the fate of a gaussian type input signal $f_{\mathrm{HPLC},i}(t)$ generated by an analyte species i taken through the GLS. As calculated with the mathemati-

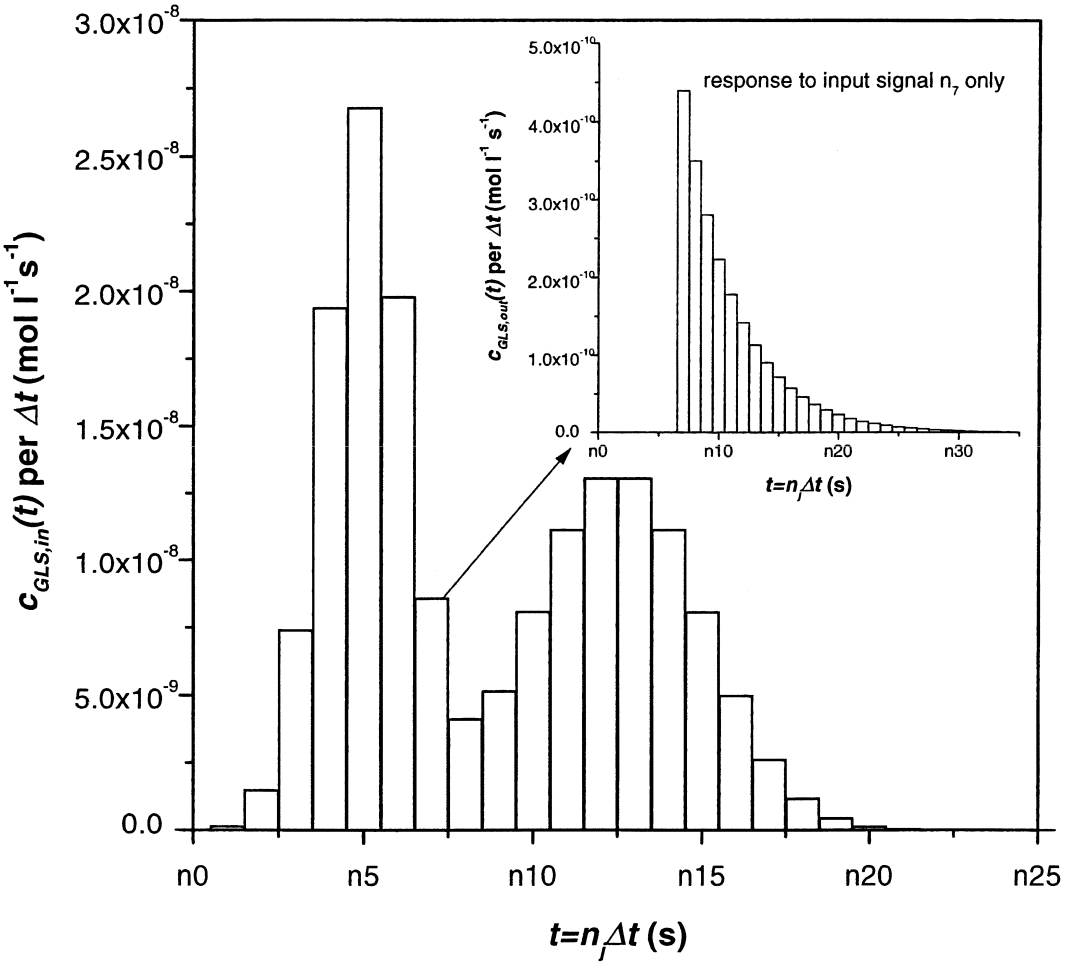

Fig. 2. Large graph, a random GLS input signal; insert, corresponding GLS output signal for input signal n_7 only.

cal model, $c_{\mathrm{GLS},i,\mathrm{out}}(t)$ shows both attenuation and tailing with respect to $c_{\mathrm{GLS},i,\mathrm{in}}(t)$. Attenuation under standard operating conditions is 0.253 ($=F_{\mathrm{H}}/(F_{\mathrm{H}}+F_{\mathrm{A}})$) due to dilution with purge gas. The $c_{\mathrm{GLS},i,\mathrm{in}}(t)$ signal has a retention time of $t_{R,i}$ whereas the $c_{\mathrm{GLS},i,\mathrm{out}}(t)$ signal has a retention time of $t_{R',i}$. The asymmetric GLS output signal $c_{\mathrm{GLS},i,\mathrm{out}}(t)$ originating from the gaussian type input signal $c_{\mathrm{GLS},i,\mathrm{in}}(t)$ is an exponentially modified gaussian (EMG) function, resulting from convolution of a gaussian type signal with an exponential decay function [16]. Data from the mathematical model were introduced into Microcal Origin Version 4.10 (Microcal Software, Northampton, USA) and fitted with the EMG fit option to establish attentuation and tailing.

2. Experimental

2.1. General

A mixture of arsenic compounds was separated on an HPLC column and detected either on-line with HG–AFS or off-line with HG–AFS after collection of discrete fractions. The arsenic compounds chosen [arsenite, As(III); arsenate, As(V); monomethylarsonic acid, MMAA] all form hydrides (arsine, AsH_3; monomethylarsine, MMA). For verification of the mathematical formulation the off-line chromatogram was subjected to Eq. (6) and compared with the on-line chromatogram. In order to be able to clearly see the deterioration effect of gas–

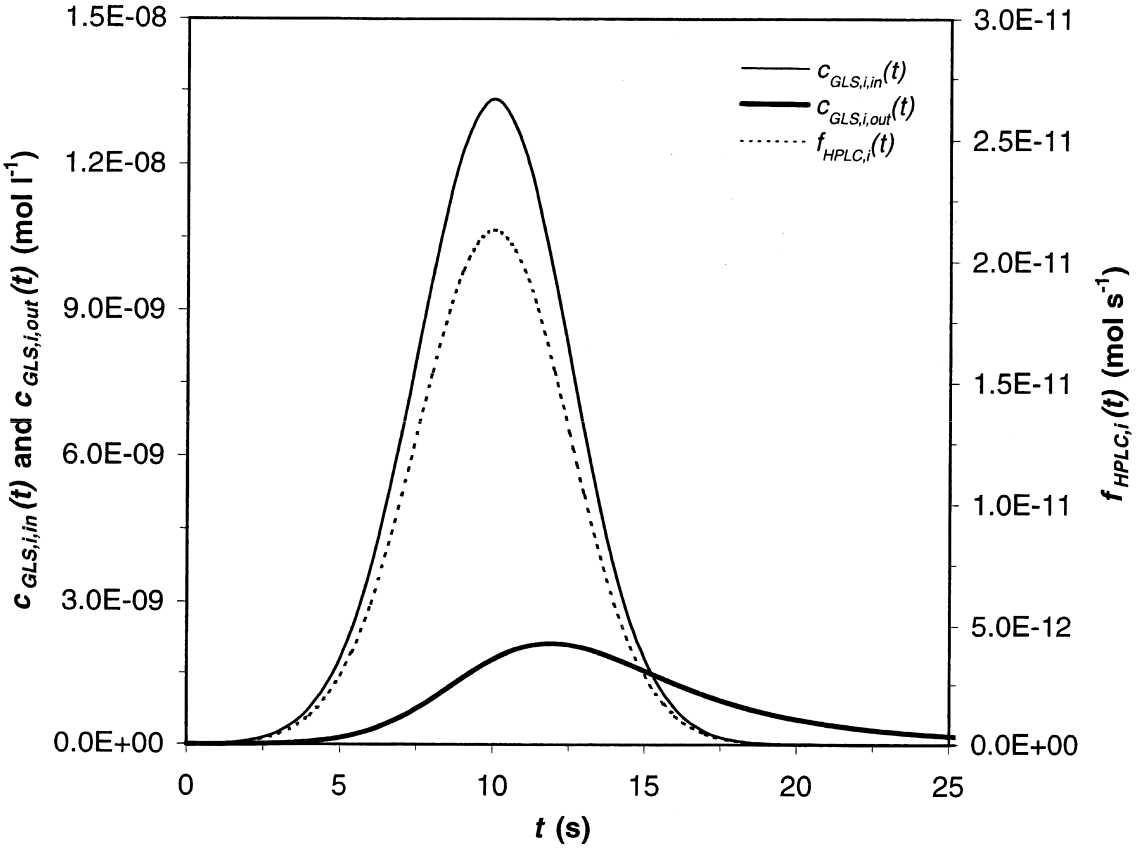

Fig. 3. Illustration of theoretical signal deterioration of a gaussian GLS input signal due to gas–liquid separation.

liquid separation, anionic arsenic compounds were separated on a cation-exchange column resulting in narrow and compressed peaks.

2.2. Separation

A mixture of arsenic compounds [As(III), As(V), MMAA] with As concentrations c_i of $1.33 \cdot 10^{-6}$ mol l^{-1} for all compounds was separated on an LKB Bromma 2150 HPLC-pump (Sweden) fitted with a Hamilton PRP-X200 cation-exchange column (0.25 m $\times$ $4.1 \cdot 10^{-3}$ m I.D.; mobile phase, $1.25 \cdot 10^{-3}$ mol l^{-1} pyridine adjusted to pH 2.65 with citric acid; volume flow-rate, $1.67 \cdot 10^{-5}$ l s^{-1}); the guard column was made of the same material as the analytical column. Samples were injected via a Rheodyne 7725i injector (Rheodyne, Cotati, CA, USA) with a sample loop V_L of 10^{-4} l.

2.3. On-line HG–AFS detection

The arsenic compounds in the HPLC effluent were mixed and reacted with hydrochloric acid (6 mol l^{-1}; $2.25 \cdot 10^{-5}$ l s^{-1}) and sodium borohydride (c_{BH} = 0.793 mol l^{-1}; $F_{BH} = 2.25 \cdot 10^{-5}$ l s^{-1}) in a high pressure PEEK (polyether ether ketone) cross (Upchurch Scientific, USA). The gas–liquid mixture was delivered to an ''A'' type gas–liquid separator (PS Analytical, Orpington, UK) with a fixed head space volume ($V_G = 2.8 \cdot 10^{-2}$ l) and the arsines generated were swept from the separator with H_2 ($F_H = 1.60 \cdot 10^{-3}$ l s^{-1}) formed from decomposition of sodium borohydride and Ar ($F_A = 4.72 \cdot 10^{-3}$ l s^{-1}). Care was taken to minimise the transfer tubing (3.0×10^{-4} l) from the HPLC system to GLS to limit signal delay and signal dispersion. The arsines were dried in a ''Perma-Pure'' mini-dryer (Perma Pure Products,

Farmingdale, USA). After drying the arsines entered the atomic fluorescence spectrometer (model Excalibur, PS Analytical) and were atomised in a hydrogen/air flame aligned in the lightpath of a boosted As hollow cathode lamp (Photron, Superlamp P803S). Since the hydrogen/air flame in the AFS detector is maintained by a constant supply of hydrogen (F_H), c_{BH} and F_{BH} were fixed (see above). The volume between GLS and flame was ca. $5 \cdot 10^{-3}$ l (mini-dryer volume and internal detector volume). Atomic fluorescence signals were retrieved with a 12 bit data acquisition card and processed with Genie Data Acquisition and Control Software (American Advantech Corp.).

2.4. Off-line HG–AFS detection

Fractions ($3.13 \cdot 10^{-2}$ g) of the HPLC effluent were collected with a fraction collector (Retriever II, Beun de Ronde, The Netherlands) and subjected to HG and AFS in a similar way as described above, i.e. via a sample loop of $2 \cdot 10^{-5}$ l the samples were measured in the flow injection mode.

3. Results and discussion

3.1. Verification of mathematical model

A chromatogram generated by flow injection–HG–AFS analysis of discrete samples of the HPLC effluent was taken through the mathematical model and the resulting ''dispersion'' chromatogram was compared with a chromatogram generated by on-line HG–AFS detection (Fig. 4). It is obvious that the ''dispersion'' chromatogram is predicted well by the mathematical model what makes it possible to further increase our understanding of parameters influencing the deterioration via mathematical modelling. The quality of the output signals is a function of the input signals [width (ratio) and resolution] and the residence time in the GLS (purge gas volume flow-rate and head space volume). The remainder of the work is a theoretical approach to predict attenuation, tailing and resolution loss of HPLC peaks simulated by gaussian signals.

3.2. Attenuation and tailing of gaussian signals as a result of gas–liquid separation

A theoretical gaussian HPLC signal $f_{HPLC,i}(t)$ for analyte species i gives rise to a gaussian hydride signal $c_{GLS,i,in}(t)$ with a retention time of $t_{R,i}$ and a width of w_i assuming negligible dispersion in the transfer from the HPLC system to GLS. When subjected to gas–liquid separation, $c_{GLS,i,in}(t)$ yields a dispersed signal $c_{GLS,i,out}(t)$ with a retention time of $t_{R',i}$ which shows both signal attenuation (A) and signal tailing (T).

Signal attenuation A for analyte species i may be defined as

$$A = \frac{c_{GLS,i,out}(t_{R',i})}{c_{GLS,i,in}(t_{R,i})} \tag{8}$$

Signal tailing T for analyte species i may be defined as

$$T = \frac{b_i}{a_i} \tag{9}$$

with a_i and b_i the peak-width parameters on the ascending and descending slope of the peak of $c_{GLS,i,out}(t)$, respectively, at 13.5% of the peak height (see Fig. 5). Variables influencing these properties are purge gas volume flow-rate (F_A) and GLS head space volume (V_G) with the width of the GLS input signal (w_i) determining the magnitude of the effect. Standard operating conditions ($F_A = 4.72 \cdot 10^{-3}$ l s^{-1}; $V_G = 2.8 \cdot 10^{-2}$ l) as mentioned in the experimental section were used to calculate the deterioration of the GLS input signal.

In Fig. 6A the attenuation as a function of F_A and V_G is given. For all three GLS input signal widths ($w_i = 5$, 10, 20 s): (1) $A = 0$ for $F_A = \infty$ with A increasing for decreasing F_A; (2) $A = 0.253$ for $V_G = 0$, denoting the dilution with purge gas ($F_H/(F_H + F_A)$), with A decreasing for increasing V_G; (3) the effect is most pronounced for the narrowest signal. For standard operating conditions A is 0.11, 0.16 and 0.21 for w_i of 5, 10 and 20 s, respectively. In Fig. 6B the tailing as a function of F_A and V_G is given. For all three GLS input signal widths ($w_i = 5$, 10, 20 s): (1) $T = 1$ for $F_A = \infty$ with T increasing for decreasing F_A; (2) $T = 1$ for $V_G = 0$ with T increasing for increasing V_G; (3) the effect is most pronounced for the

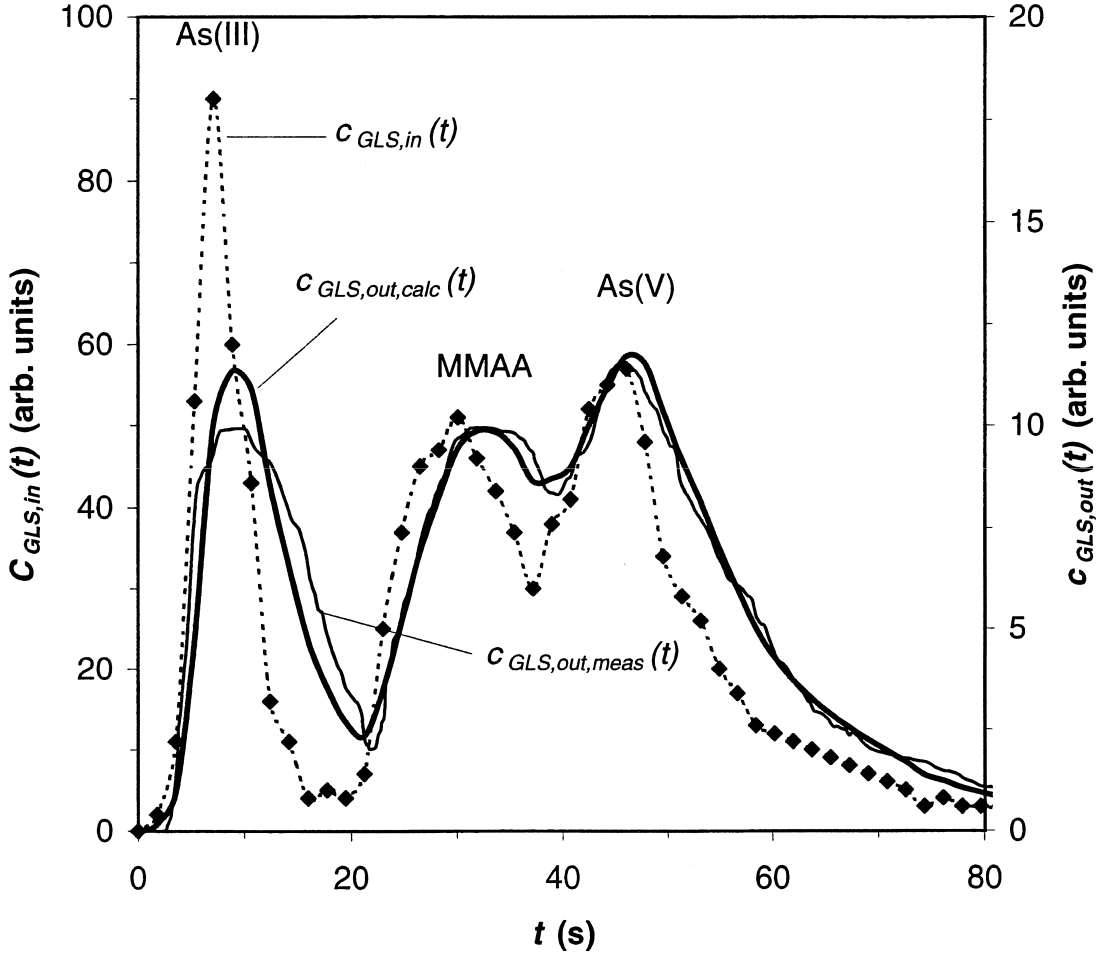

Fig. 4. HPLC chromatograms [separation of As(III), As(V) and MMAA]: GLS input $c_{GLS,in}(t)$ (discrete samples from HPLC effluent) and calculated and measured GLS output $c_{GLS,out,calc}(t)$ and $c_{GLS,out,meas}(t)$.

narrowest signal. For standard operating conditions T is 2.99, 1.79 and 1.27 for w_i of 5, 10 and 20 s, respectively. It is obvious that minimising V_G results in both minimal signal attenuation and signal tailing; for F_A there is a trade-off between signal attenuation and signal tailing, e.g. minimising F_A results in maximal signal attenuation and minimal signal tailing and vice versa.

3.3. Influence of GLS on resolution of gaussian signals

Two neighbouring theoretical gaussian HPLC signals $f_{HPLC,1}(t)$ and $f_{HPLC,2}(t)$ give rise to two neighbouring gaussian hydride signals $c_{GLS,1,in}(t)$ and $c_{GLS,2,in}(t)$. Assuming negligible dispersion in the transfer from the HPLC system to GLS, retention times of $t_{R,1}$ and $t_{R,2}$ and widths of w_1 and w_2 yield a GLS input resolution R_{in} of

$$R_{in} = \frac{t_{R,2} - t_{R,1}}{2 \cdot (w_1 + w_2)} \quad (10)$$

When subjected to gas–liquid separation, two neighbouring non-symmetrical hydride output signals $c_{GLS,1,out}(t)$ and $c_{GLS,2,out}(t)$ are obtained with retention times of $t_{R',1}$ and $t_{R',2}$ and peak-width parameters of b_1 and a_2 (see Fig. 5). The GLS output resolution R_{out} may be defined as [17]

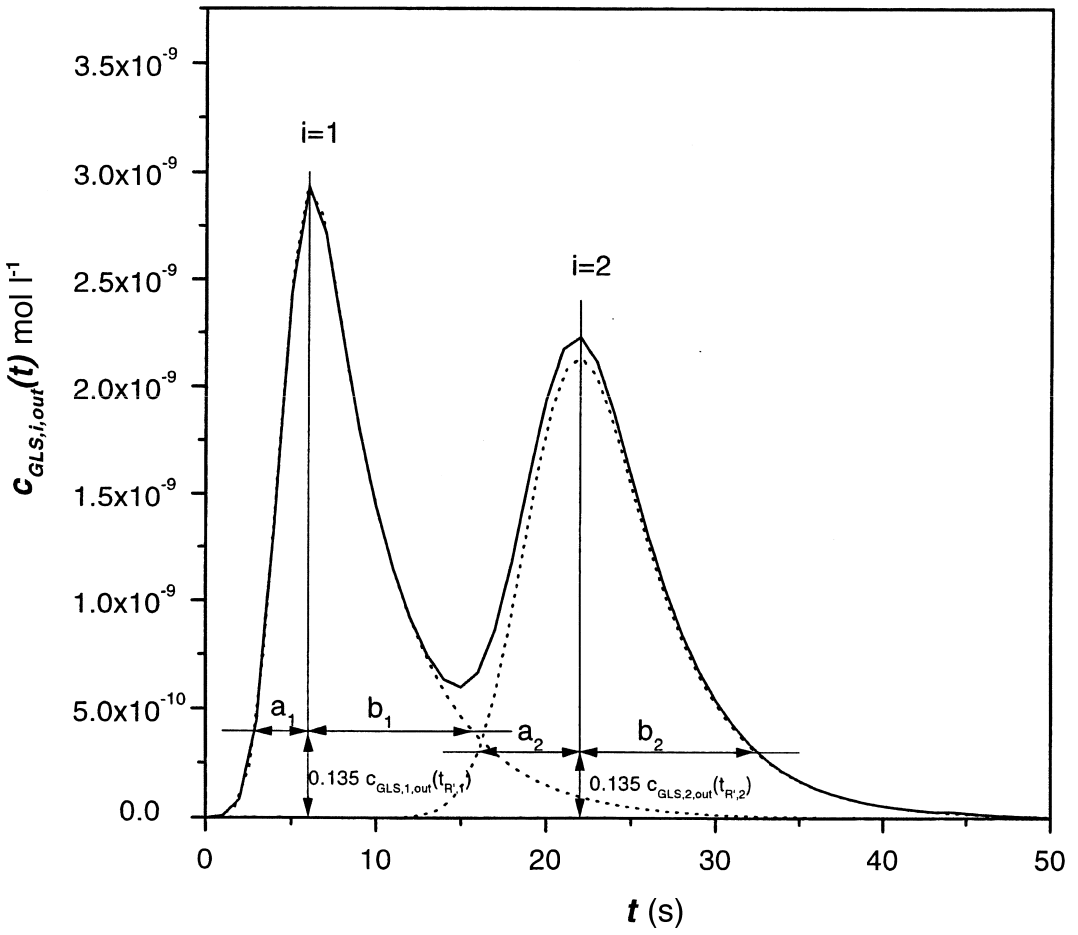

Fig. 5. Illustration of the definition of tailing (T) and resolution (R); the solid line denotes the GLS output and the dotted lines represent the deconvoluted peaks obtained by fitting with two EMG functions; peak-width parameters a_i and b_i determine T and R (see text).

$$R_{\text{out}} = \frac{t_{R',2} - t_{R',1}}{b_1 + a_2} \tag{11}$$

with $R_{\text{out}} \leq R_{\text{in}}$.

Under standard operating conditions as mentioned in the experimental section ($F_A = 4.72 \cdot 10^{-3}$ l s^{-1}; $V_G = 2.8 \cdot 10^{-2}$ l; $V_L = 10^{-4}$ l), loss of signal resolution due to gas–liquid separation was calculated for neighbouring gaussian input hydride peaks with GLS input resolutions R_{in} of 0.75, 1 and 1.25. Assuming input signal ratios of 1 ($c_1 = c_2 = 1.33 \cdot 10^{-6}$ mol l^{-1}) and input widths of 10 s ($w_1 = w_2$), Fig. 7 visualises these calculations and shows the detrimental effect of gas–liquid separation on the GLS output resolution R_{out}, especially at small GLS input resolutions. For the three input signals a, b and c, the GLS output resolution was 0.45, 0.60 and 0.75, respectively.

To enhance the GLS output resolution, the HPLC separation characteristics and/or the gas–liquid separation variables may be optimised. For the HPLC separation characteristics it is obvious that better resolved peaks yield a better R_{out} and thus optimisation of the separation conditions (column type, mobile phase composition) should be the first aim. However, also the width of the peaks plays an important role in resolution loss due to gas–liquid separation as will be illustrated below.

When plotting R_{out} vs. R_{in} for the output and input signals from Fig. 7, a linear relationship is found as

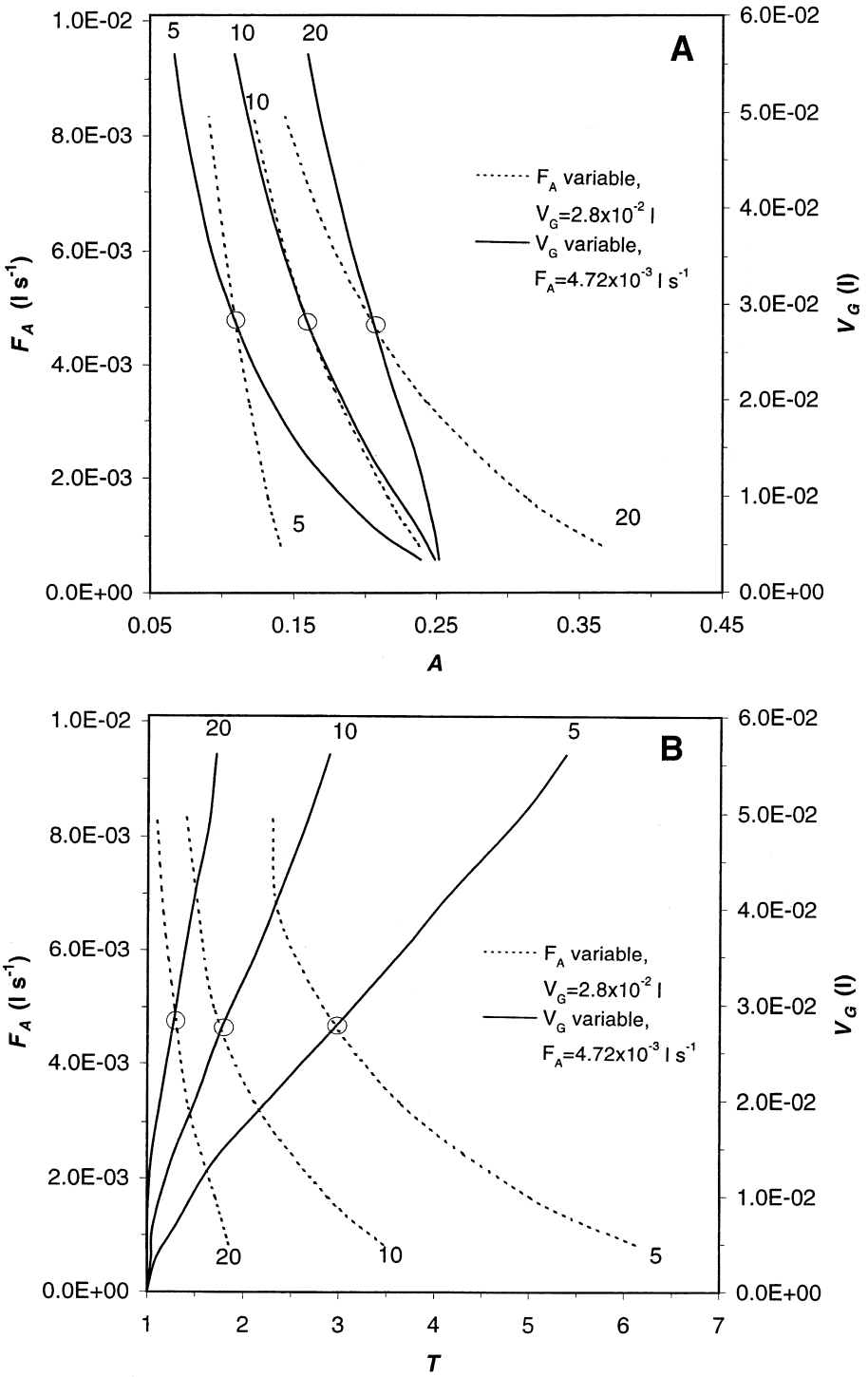

Fig. 6. Attenuation (A) and tailing (B) of gaussian GLS input signals with different widths (w_i=5, 10 and 20 s) as a function of F_A and V_G; F_H=1.6·10^{-3} l s^{-1}; c_i=1.33·10^{-6} mol l^{-1}; circles mark attenuation and tailing for the different widths under standard operating conditions.

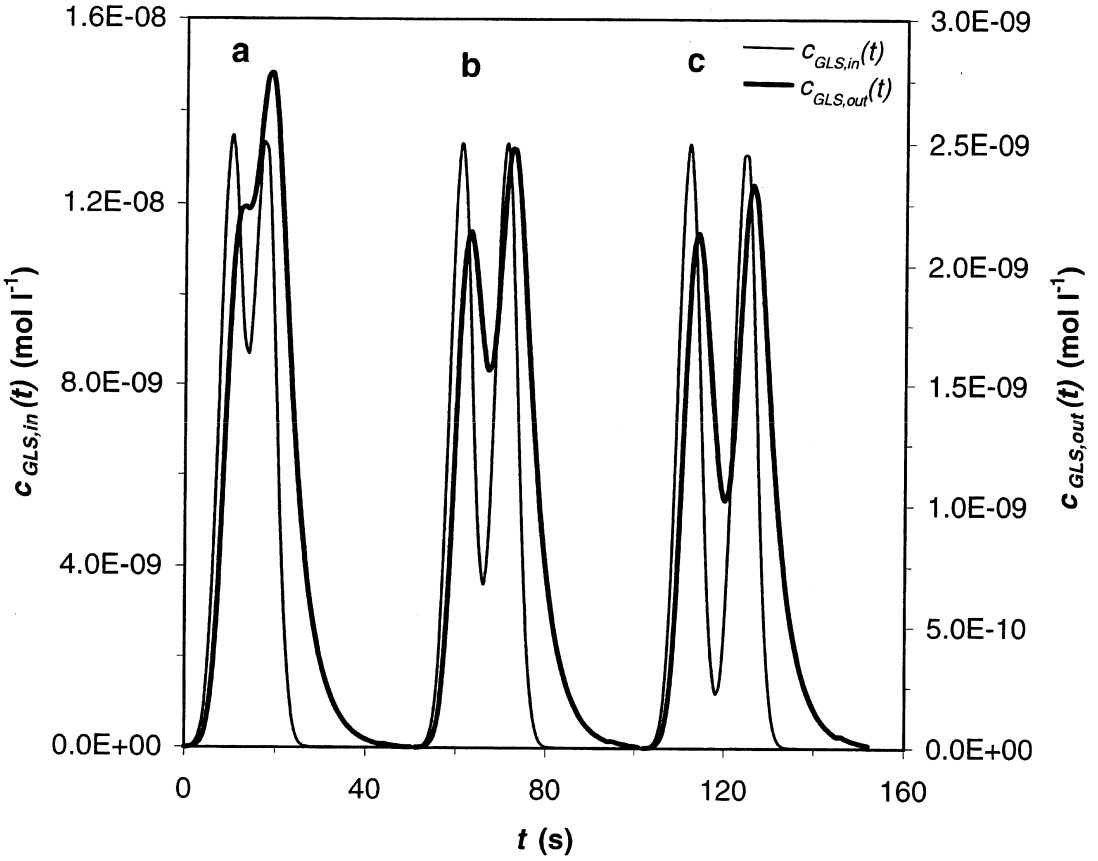

Fig. 7. Illustration of resolution loss due to gas–liquid separation as a function of GLS input resolution (a, $R_{in}=0.75$; b, $R_{in}=1$; c, $R_{in}=1.25$); input signals are gaussian functions and output signals are exponentially modified gaussian functions; $w_1=w_2=10$ s; $c_1=c_2=1.33\cdot10^{-6}$ mol l^{-1}.

can be observed from Fig. 8A ($w_1=w_2=10$ s); the same is valid for input widths of 5 and 20 s ($w_1=w_2$). This implies that the resolution loss of two neighbouring gaussian input signals ($w_1=w_2$) is independent of the GLS input resolution R_{in}. The resolution loss factor R_{out}/R_{in} can be calculated from the slopes of the graphs in Fig. 8A and is presented in Fig. 8B ($w_1=w_2=10$ s); the other two graphs ($w_1=2w_2$ and $w_1=0.5w_2$) represent cases where the width of the first peak is double or half that of the second peak. As can be seen, a gradual increase in peak widths results in less resolution loss in all cases, but there is a significant difference whether the first or second peak is wider. This is indicated in Fig. 8B for two w_1:w_2 peak width situations, viz. 10:20 and 20:10, giving R_{out}/R_{in} values of 0.687 and 0.749, respectively. This is understandable as a wider first peak shows less carry-over to the second peak and thus less influence on the GLS input resolution is seen.

Furthermore, the GLS output resolution may be enhanced by optimisation of the residence time τ ($=V_G/(F_A+F_H)$). In Fig. 9 the resolution loss R_{out}/R_{in} as a function of τ is given assuming input signal ratios of 1 ($c_1=c_2=1.33\cdot10^{-6}$ mol l^{-1}) and gaussian GLS input signal widths of 5, 10 and 20 s ($w_1=w_2$). For all three GLS input signal widths: (1) $R_{out}/R_{in}=1$ for $\tau=0$ ($F_A=\infty$ and/or $V_G=0$) with R_{out}/R_{in} increasing for decreasing τ (increasing F_A and/or decreasing V_G); (2) the effect is most pronounced for the narrowest signals. For standard operating conditions R_{out}/R_{in} is 0.39, 0.60 and 0.80

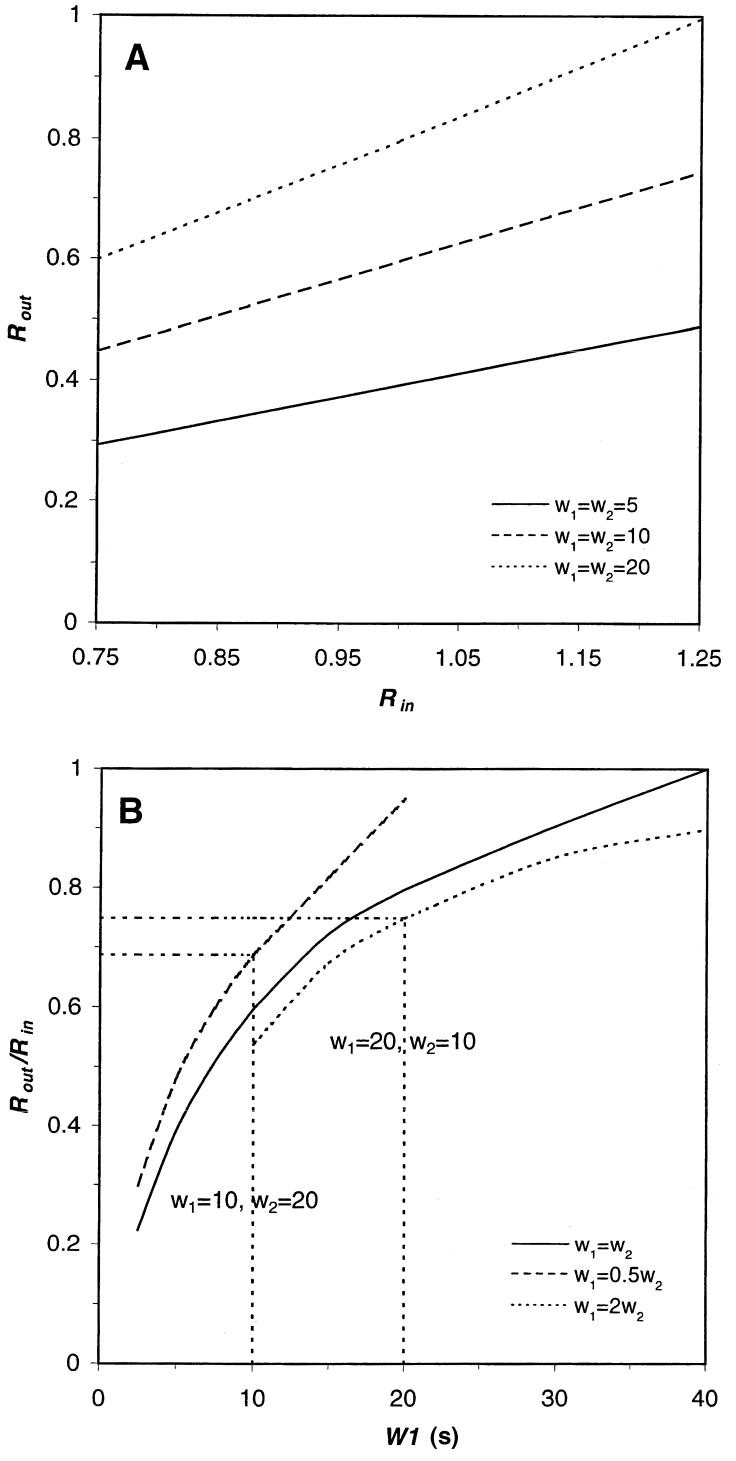

Fig. 8. (A) Output resolution R_{out} as a function of input resolution R_{in} for different gaussian GLS input widths ($w_1=w_2$); (B) Resolution loss R_{out}/R_{in} as a function of different gaussain GLS input width ratios ($w_1=w_2$, $w_1=2w_2$, $w_1=0.5w_2$); $c_1=c_2=1.33\cdot10^{-6}$ mol l^{-1}. In all cases the width is given in s.

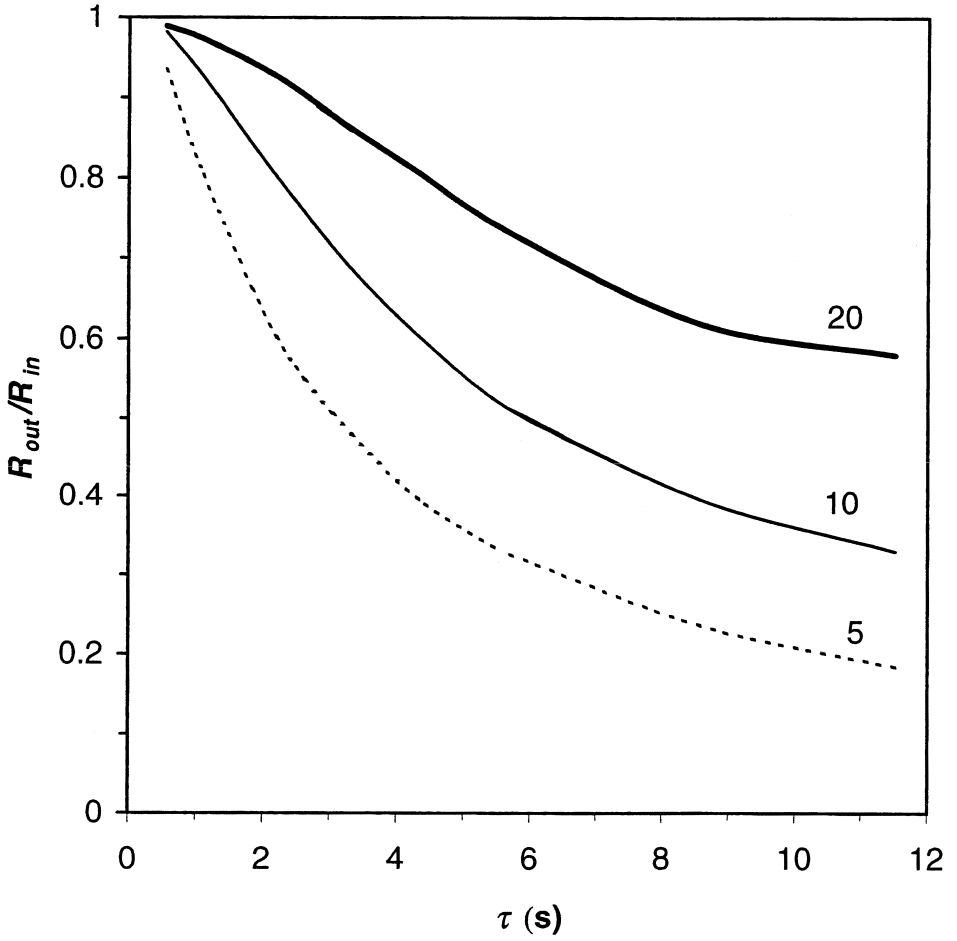

Fig. 9. Resolution loss R_{out}/R_{in} of neighbouring gaussian GLS input signals ($w_1 = w_2$) with widths of 5, 10 and 20 s as a function of residence time τ ($=V_G/(F_A+F_H)$) in the GLS; $F_H = 1.6 \cdot 10^{-3}$ l s^{-1}; $c_1 = c_2 = 1.33 \cdot 10^{-6}$ mol l^{-1}.

for input widths ($w_1 = w_2$) of 5, 10 and 20 s, respectively.

4. Conclusions

The mathematical model describes the behaviour of HPLC peaks in the gas–liquid separation interface well as verified experimentally in a set-up comprising HPLC–HG–AFS for arsenic speciation. This makes it possible to predict peak deterioration (attenuation, tailing, resolution loss) due to a hydride generation interface in a hyphenated speciation system as a function of the characteristics of the input peaks [width (ratio) and resolution] and the gas–liquid separation variables (gas–liquid separator head space volume and purge gas volume flow-rate) using gaussian signals for simulation of HPLC peaks.

It follows that a minimal gas–liquid separator head space volume is beneficial in all instances whereas the purge gas volume flow-rate is a compromise between attenuation on the one hand and tailing and resolution loss on the other hand. Lowering the purge gas volume flow-rate results in less attenuation and more tailing and resolution loss and vice versa. The width (ratio) and resolution of HPLC signals is critical for the magnitude of the effect with

narrow signals, close to each other, the first one narrower than the second one, to be the most susceptible to deterioration.

5. Symbols

i	Analyte species
c_i	Concentration of analyte species i (mol l^{-1})
V_L	Sample loop volume (l)
E_i	Reduction efficiency of analyte species i
F_A	Volume flow-rate of argon (l s^{-1})
F_H	Volume flow-rate of hydrogen (l s^{-1})
F_{BH}	Volume flow-rate of borohydride (l s^{-1})
c_{BH}	Concentration of borohydride (mol l^{-1})
V_G	GLS head space volume (l)
$f_{HPLC}(t)$	Total mass flow-rate of analyte species from HPLC (mol s^{-1})
$c_{GLS,in}(t)$	Total concentration of hydrides entering GLS (mol l^{-1})
$c_{GLS,out}(t)$	Total concentration of hydrides leaving GLS (mol l^{-1})
w_i	Width of peak i at 13.5% of peak height (s)
$t_{R,i}$	Retention time of peak i entering GLS (s)
$t_{R',i}$	Retention time of peak i leaving GLS (s)
A	Attenuation
T	Tailing
R_{in}	Resolution of peaks entering GLS
R_{out}	Resolution of peaks leaving GLS

Acknowledgements

The authors would like to thank Professor Dr. Ir. J.J.M. de Goeij for constructive discussions and Ms. T.G. Verburg for assistance with the mathematical modelling.

References

[1] B. Welz, Spectrochim. Acta, Part B 53 (1998) 169.
[2] G.K. Zoorob, J.W. McKiernan, J.A. Caruso, Mikrochim. Acta 128 (1998) 145.
[3] E.H. Larsen, G.A. Pedersen, J.W. McLaren, J. Anal. At. Spectrom. 12 (1997) 963.
[4] P. Kavanagh, M.E. Farago, I. Thornton, W. Goessler, D. Kuehnelt, C. Schlagenhaufen, K.J. Irgolic, Analyst 123 (1998) 27.
[5] A. Sanz-Medel, Analyst 120 (1995) 799.
[6] A.G. Howard, J. Anal. At. Spectrom. 12 (1997) 267.
[7] J. Lintschinger, P. Schramel, A. Hatalak-Rauscher, I. Wendler, B. Michalke, Fresenius J. Anal. Chem. 362 (1998) 313.
[8] C. Demesmay, M. Olle, M. Porthault, Fresenius J. Anal. Chem. 348 (1994) 205.
[9] X.-C. Le, W.R. Cullen, K.J. Reimer, Talanta 41 (1994) 495.
[10] K.J. Lamble, S.J. Hill, Anal. Chim. Acta 334 (1996) 261.
[11] J.L. Gomez-Ariza, D. Sánchez-Rodas, R. Beltran, W. Corns, P. Stockwell, Appl. Organomet. Chem. 12 (1998) 1.
[12] Z. Šlejkovec, J.T. van Elteren, A.R. Byrne, J.J.M. de Goeij, Anal. Chim. Acta 380 (1999) 63.
[13] X. Zhang, R. Cornelis, J. de Kimpe, L. Mees, Anal. Chim. Acta 319 (1996) 177.
[14] M. Johansson, M. Berglund, D.C. Baxter, Spectrochim. Acta, Part B 48 (1993) 1393.
[15] J.T. van Elteren, Z. Šlejkovec, H.A. Das, Spectrochim. Acta, Part B 54 (1999) 311.
[16] M.S. Jeansonne, J.P. Foley, J. Chromatogr. Sci. 29 (1991) 258.
[17] P.J. Schoenmakers, J. Chromatogr. 458 (1988) 355.